Supplemental Information

Table S1. Metabolic pathways changed by KSHV compared to uninfected TIME cells in 3D culture.

Significantly affected metabolic pathway by KSHV with cut-off with impact >0.15 and p-value <0.05 are considered the most influenced pathways in TIME cells.

Table S2. Metabolic pathways changed by KSHV compared to uninfected MCF10A cells in 3D culture.

Significantly affected metabolic pathway by KSHV with cut-off with impact >0.15 and p-value <0.05 are considered the most influenced pathways in MCF10A cells.

Table S3. Peptides of PYCR identified by mass spectrometry.

Table S4. Primers list for qPCR.

Fig. S1. Heat maps and PCA plots of metabolites in control and KSHV infected cells.

(A) Clustered heatmap depicting levels of 176 metabolites in TIME cells, 165 metabolites in MCF10A cells. Columns indicate samples from 2D grown Mock or KSHV infected cells or 3D grown Mock or KSHV infected cells. Rows depict individual metabolites. (B) Principal component PCA score plots reveal separation in metabolite profiles between samples.

Fig. S2. *PYCR* alteration profile in various cancer samples.

(A) *PYCR1* and (B) *PYCR2* alterations (Mutation, Deletion, Amplification) were detected and visualized from cBioPortal.

Fig. S3. K1-PYCR interaction and mapping.

(A) A series of GST-K1 cytoplasmic region mutants depicted in the upper panel were transfected into HEK293T cells. Cell lysates were used for GST PD, followed by immunoblotting with anti-PYCR1, anti-PYCR2 and anti-GST antibodies. (B) A series of GST-PYCR2 truncated mutants depicted in the upper panel were co-transfected with full-length K1 in HEK293T cells. Cell lysates were then applied to GST-PD, followed by immunoblotting with anti-PYCR1, anti-PYCR2 and anti-GST antibodies. (C) *In vitro* GST-PD assay. Purified GST-K1(C) and GST-K1(C)pY proteins from *E. coli* TKX1 strain were stained by Coomassie blue and their tyrosine phosphorylation were examined with anti-phosphotyrosine (p-Tyr) antibody. Purified His-tagged PYCR2 (His-PYCR2) were incubated with GST, GST-K1(C) or GST-K1(C)pY for GST-PD. Input represents 10% of samples used *in vitro* binding assay. Arrowhead indicates the His-PYCR2 and asterisks indicate GST, GST-K1 and GST-K1(C)pY. (D) The cytoplasmic domain of K1 A, B, C and D subtypes fused with GST depicted in the upper panel were transfected into HEK293T cells. Cell lysates were used for GST-PD, followed by immunoblotting with anti-PYCR1, anti-PYCR2 and anti-GST antibodies. (E) The cytoplasmic domain of LMP2, R1, and K1 fused with GST were transfected into HEK293T cells. Cell lysates were used for GST-PD, followed by immunoblotting with anti-PYCR1, anti-PYCR2 and anti-GST antibodies.

Fig. S4. Mitochondria localization of K1 B, C and D subtypes.

(A) Subcellular fractionation of mock- or K1-transfected HEK293T cells to cytosolic (Cyto), plasma membrane (PM), mitochondrial (Mito) and nuclear (Nu) fractions. K1 was detected by immunoblotting with anti-K1 antibody. Arrowhead indicates 46 kDa K1 and asterisk indicates 70 kDa glycosylated K1. Mitofillin, β-actin, Histone H3 and Na-K-ATPase were used as organelle-specific markers of mitochondria, cytosol, nucleus, and plasma membrane respectively. (B) Representative confocal fluorescence images of K1 subtypes in Hela cell. At 48 hours of transfection of the C-terminal Flag-tagged K1, Hela cells were stained with mitotracker, anti-PYCR2 antibody and anti-K1 antibody. Merged images of K1 (Red) and PYCR2 (Green) and nucleus (Blue). Scale bar=10 μm.

Fig. S5. Expression of K1 in 2D and 3D culture.

(A) TIME and (B) MCF10A cells cultured in 2D and 3D condition were harvested to determine KSHV gene expression by RT-qPCR. Data represents normalized (with actin mRNA) fold change (3D/2D). Data are presented as the mean ± SEM. *, $P < 0.05$; **, $P < 0.01$; ***, $P= 0.0002$, by Student's t test.

Fig. S6. Relative abundance of metabolites in proline metabolic pathway measured by LC-MS.

Fold changes in metabolite associated with proline metabolic pathway in Mock, KSHV WT infected and KSHV K1ΔC infected TIME cells. The level of each metabolite in Mock cells was set at 1. Data are mean ± SD. *, $P < 0.05$; **, $P < 0.01$, by 1-way ANOVA.

Fig. S7. K1 expression in TIME, MCF10A and MDA-MB-231 cells and PYCR1/2 knockdown in TIME and KMM cells.

(A) Immunoblotting analysis of K1 and mutant expression in TIME cells. (B) Proliferation rate of mock-, K1 WT-, or mutant-overexpressing TIME cells in 2D monolayer. Proliferation was measured by counting the cell numbers. Data are presented as the mean ± SEM. (C) Immunoblotting analysis of K1 and mutant expression in MCF10A cells. (D) Proliferation rate of mock-, K1 WT-, or mutant-overexpressing MCF10A cells in 2D monolayer. Proliferation was measured by counting cell numbers. Data are presented as mean ± SEM. (E) Immunoblotting analysis of K1 and mutant expression in MDA-MB-231. (F) Proliferation rate of mock-, K1 WT-, or mutant-overexpressing MDA-MB-231 cell in 2D monolayer. Proliferation was measured by counting the cell numbers. Data are presented as the mean ± SEM. (G) Immunoblotting analysis of K1, K1 mutant or PYCR1/2 expression in TIME cells transfected with scramble shRNA control or PYCR-specific shRNA. β-Actin was used as loading control. (H) Proliferation rate of mock-, K1 WT-, or mutant-overexpressing and/or PYCR1/2-knockdown TIME cells in 2D monolayer. Proliferation was measured by counting the cell number. Data are presented as the mean ± SEM. (I) Immunoblotting analysis of PYCR1/2 expression in scramble shRNA- or PYCR-specific shRNA-treated KSHV infected TIME cells (J) KMM cells.

Fig. S8. 3D hydrogel scaffolds for endothelial cell growth.

(A) 3D printed hydrogel scaffolds designed to feature the shape of a hexagonal prism (diagonal length: 3 mm; height: 3 mm) consisting of parallel microchannels (diameter: 150 μm) Scale bar: 500 μm. (B) Schematic diagram depicting 3D cell culture in the hydrogel scaffolds.

Fig. S9. Targeted metabolomics profile of mock-, K1 WT- or mutant-expressing MDA-MB-231 tumors from nude mice.

Heat map generated from $\log_2$ value of fold-change compared to mock tumors (n = 3-4).

Table S1. Metabolic pathways changed by KSHV compared to uninfected TIME cells in 3D culture.

Pathway	P-value	Impact
Alanine, aspartate and glutamate metabolism	0.000013073	0.48718
Cysteine and methionine metabolism	0.0017537	0.1703
Arginine and proline metabolism	0.0019014	0.28937
Thiamine metabolism	0.017911	0.15346
Pantothenate and CoA biosynthesis	0.024622	0.18014
D-Glutamine and D-glutamate metabolism	0.026424	0.28342

Table S2. Metabolic pathways changed by KSHV compared to uninfected MCF10A cells in 3D culture.

Pathway	P-value	Impact
Glutathione metabolism	0.00011031	0.26552
Taurine and hypotaurine metabolism	0.00067474	0.36331
Alanine, aspartate and glutamate metabolism	0.0013899	0.54416
Glycine, serine and threonine metabolism	0.0030097	0.18845
Arginine and proline metabolism	0.0050402	0.23591

Table S3. Peptides of PYCR identified by mass spectrometry.

Bands	Protein	Total Peptides	Peptides detected
P35	PYCR1	21	(R) ELQSMADQEQVSPAAIK
			(K) IMASSPDMDLATVSALR
			(R) EGATVYATGTHAQVEDGR
			(K) VKLDSPAGTALSPSGHTK
			(F) ILDEIGADIEDR
			(R) HIVVSCAAGVTISSIEK
			(F) TALDALADGGVK
			(R) ELQSMADQEQVSPAAIK
			(K) MLLHSEQHPGQLK
			(K) LDSPAGTALSPSGHTK
			(K) GFTAAGVLAAHK
			(F) TAAGVLAAHK
			(F) ILDEIGADIEDR
			(K) DNVSSPGGATIHALHVLESGGFR
	PYCR2	2	(R) LGAQALLGAAK
			(R) SLLINAVEASCIR
P32	PYCR1	2	(R) ELQSMADQEQVSPAAIK
			(K) MLLHSEQHPGQLK
	PYCR2	1	(R) SLLINAVEASCIR

Table S4. List of primers used in this study.

Gene	Primer
Actin_F	CCACAGCCAGAGGTCCTCAG
Actin_R	AGGAGCTCTTGGAGGGCATG
K1_F	TACGCTGATGGACCAAACGG
K1_F	ACGCGCCGAAAAACATAGAC
LANA_F	GAAGTGGATTACCCTGTTGTTAGC
LANA_R	TTGGATCTCGTCTTCCATCC
ORF36_F	ATTGCCAACGACCTGATGCA
ORF36_R	ACTCCAGTCCAGCTGCAGCA
ORF57_F	AGGGATATCACCGCTCTCATAAGA
ORF57_R	CTGCGGTTTCTCGACGGCAACTCA
RTA_F	CACAAAAATGGCGCAAGATGA
RTA_R	TGGTAGAGTTGGGCCTTCAGTT

Fig. S1. Heat maps and PCA plots of metabolites in control and KSHV infected cells

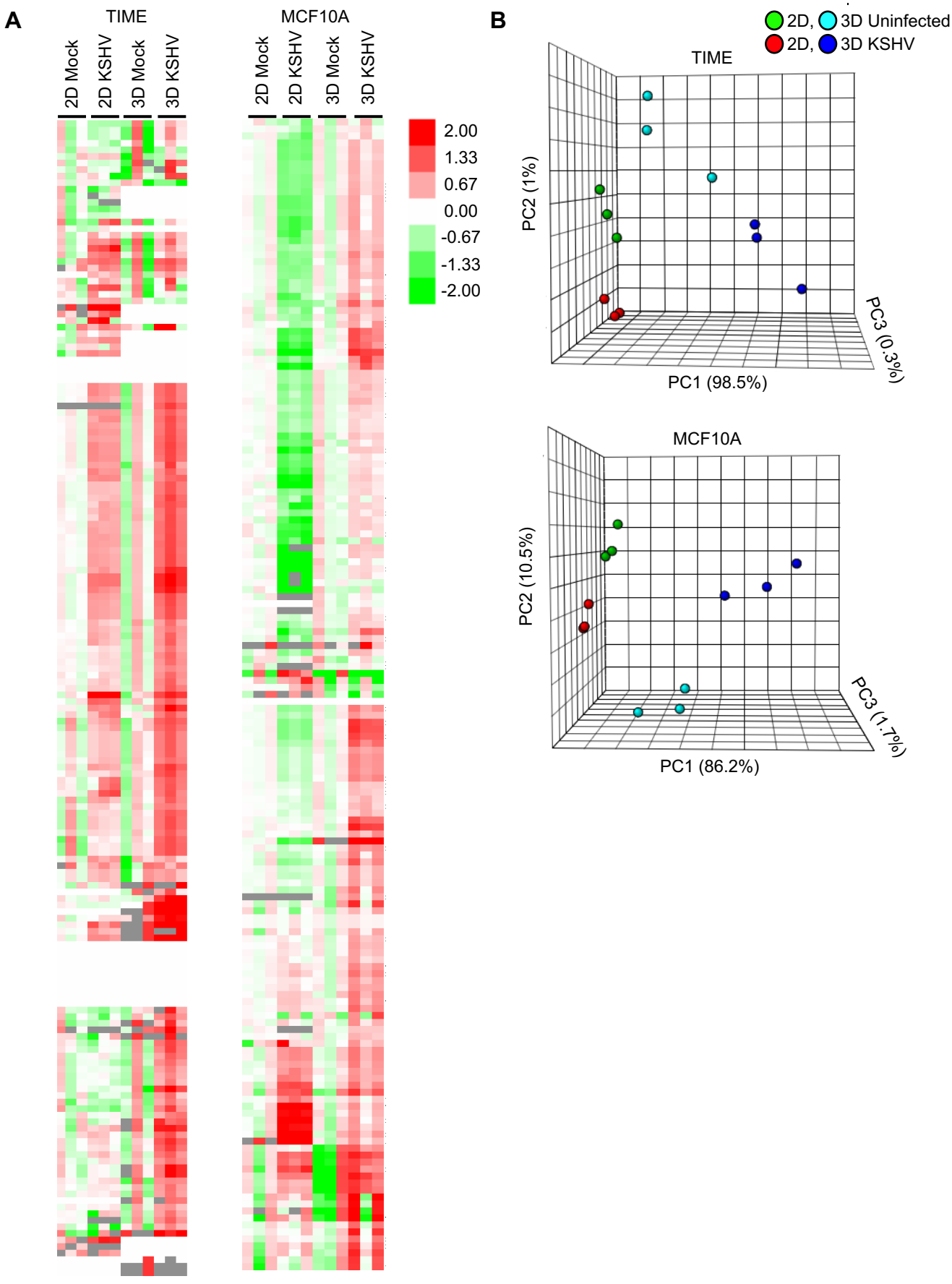

Fig. S2. *PYCR* alteration profile in various cancer samples

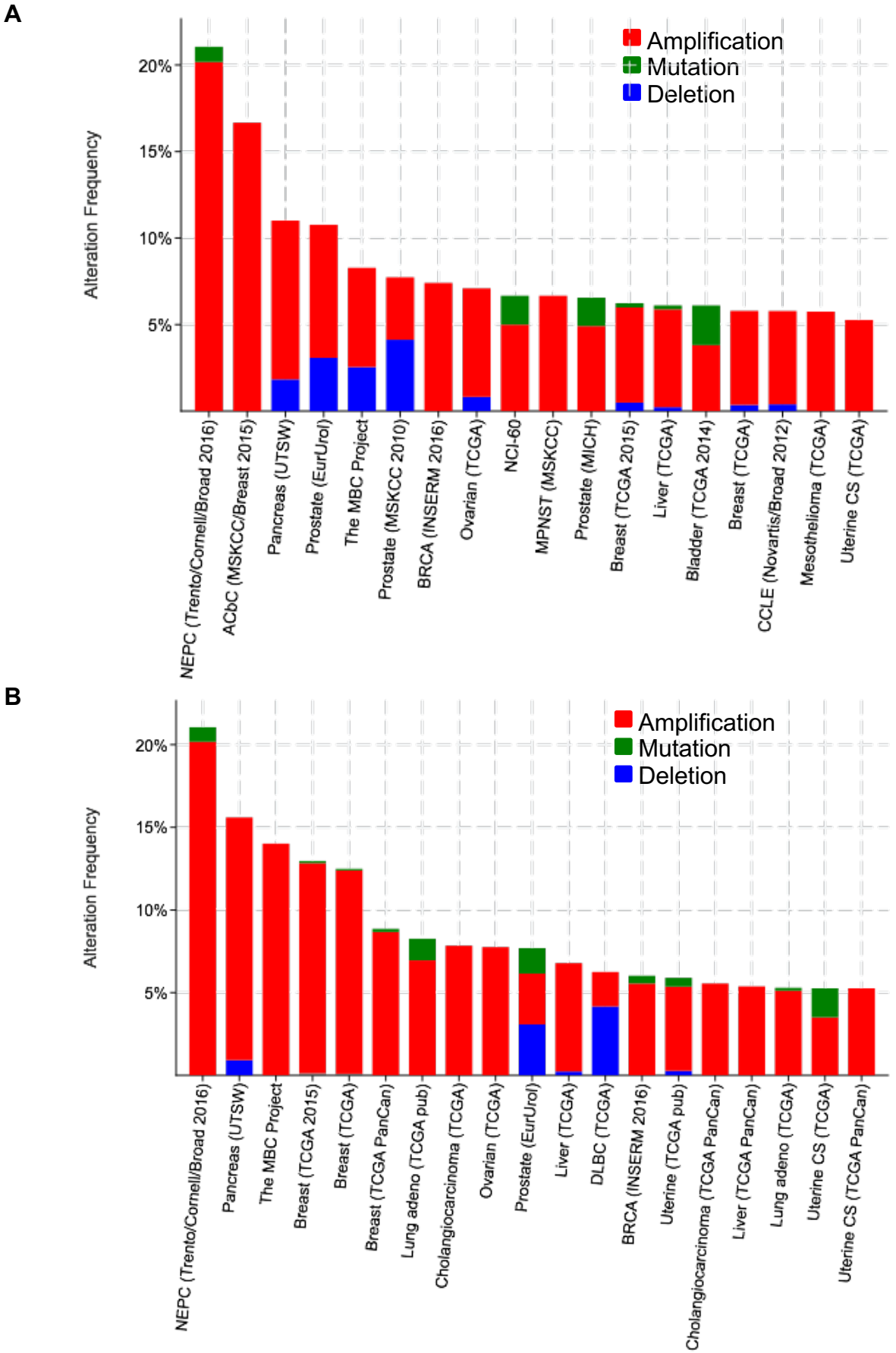

Fig. S3. K1-PYCR interaction and mapping

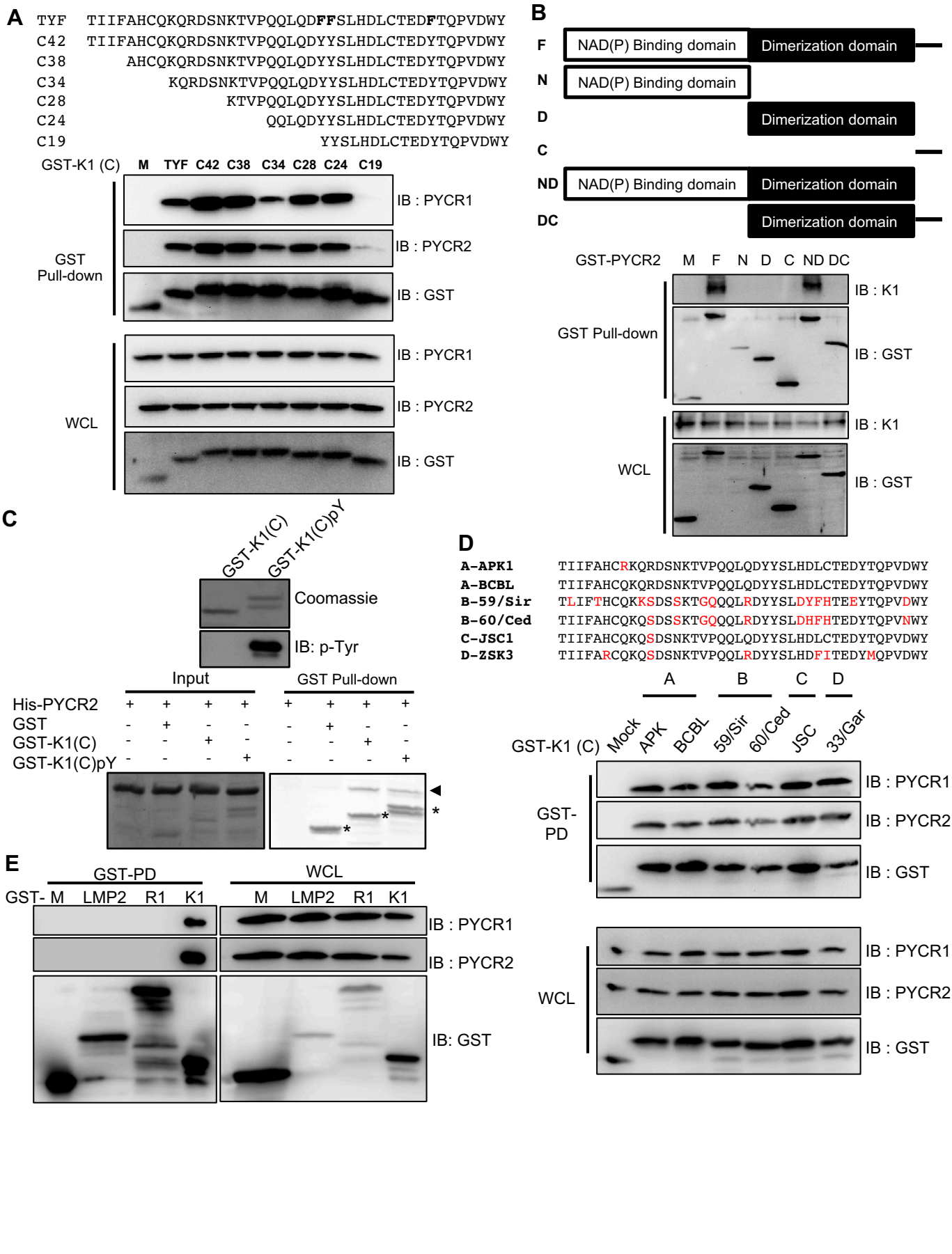

Fig. S4. Mitochondria localization of K1 B,C and D subtypes

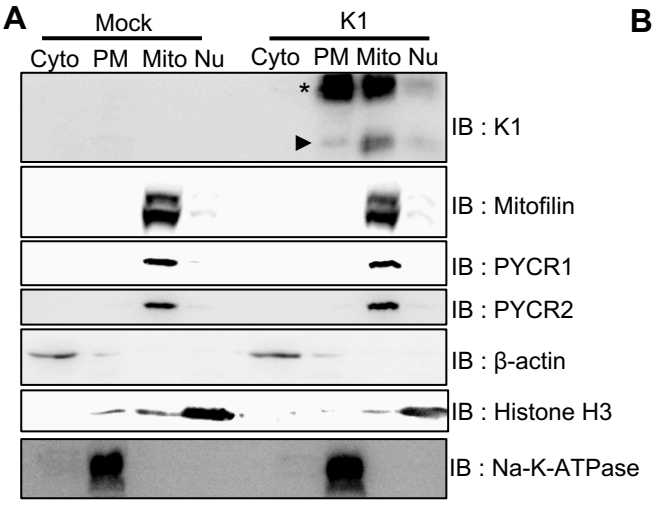

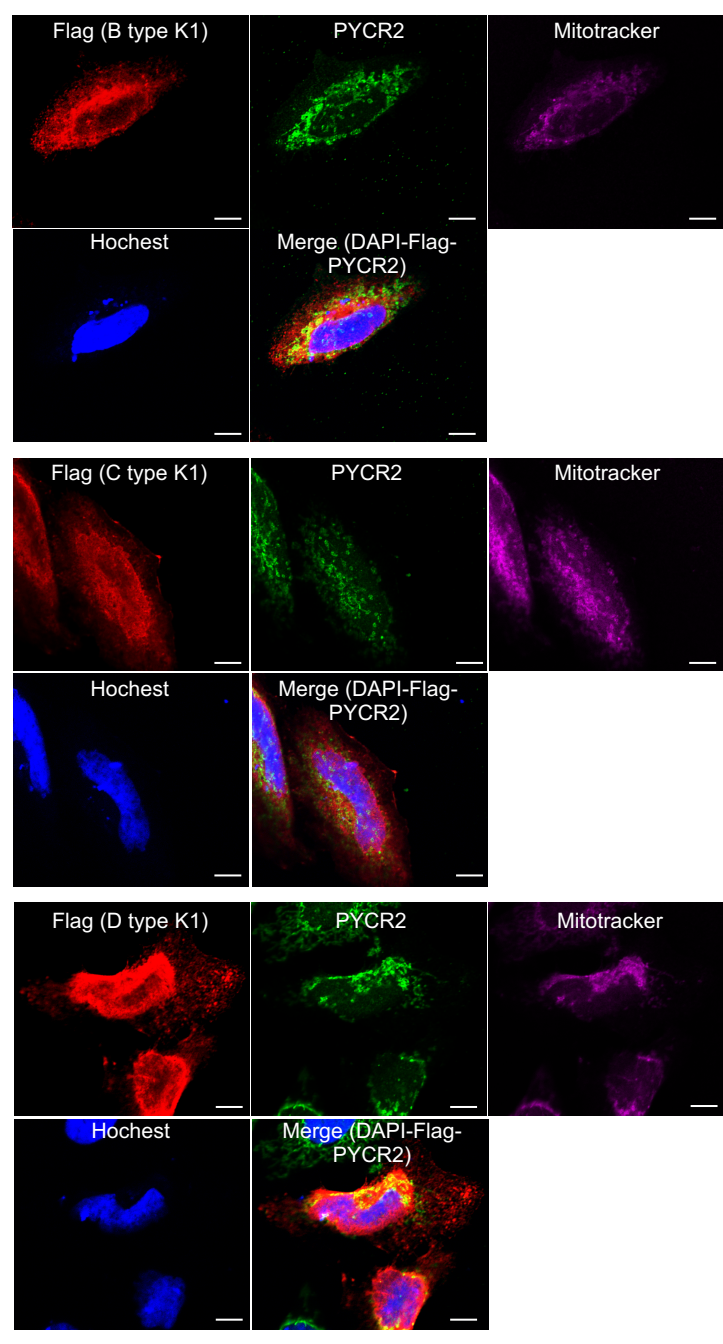

Fig. S5. Expression of K1 in 2D and 3D culture

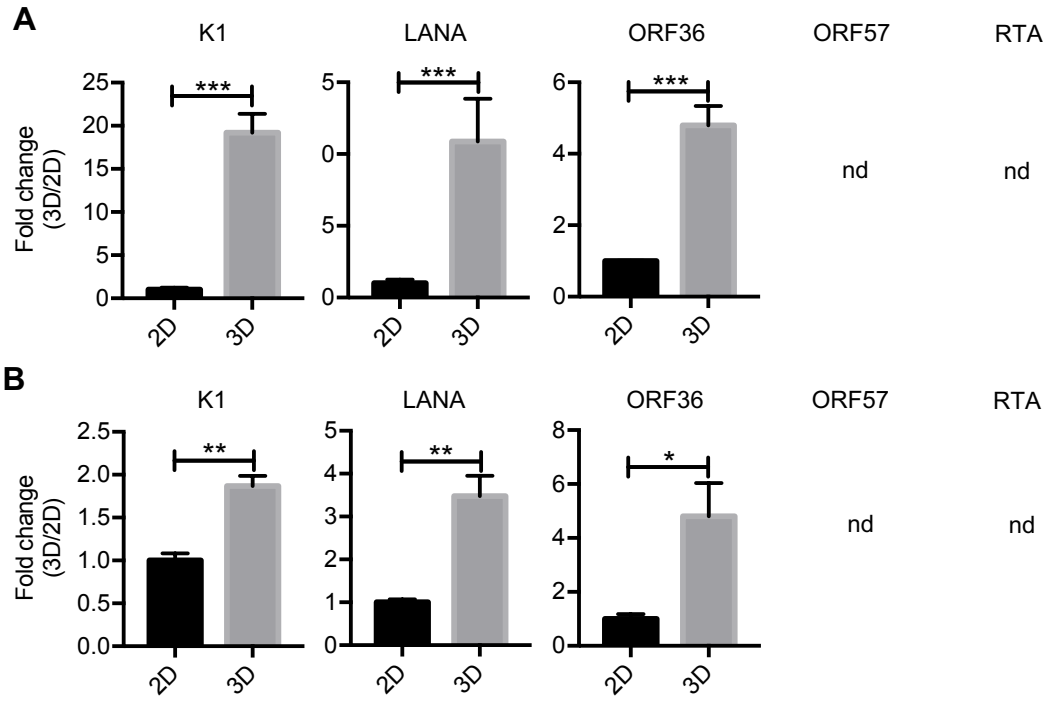

Fig. S6. Relative content of metabolites in proline metabolic pathway measured by LC-MS

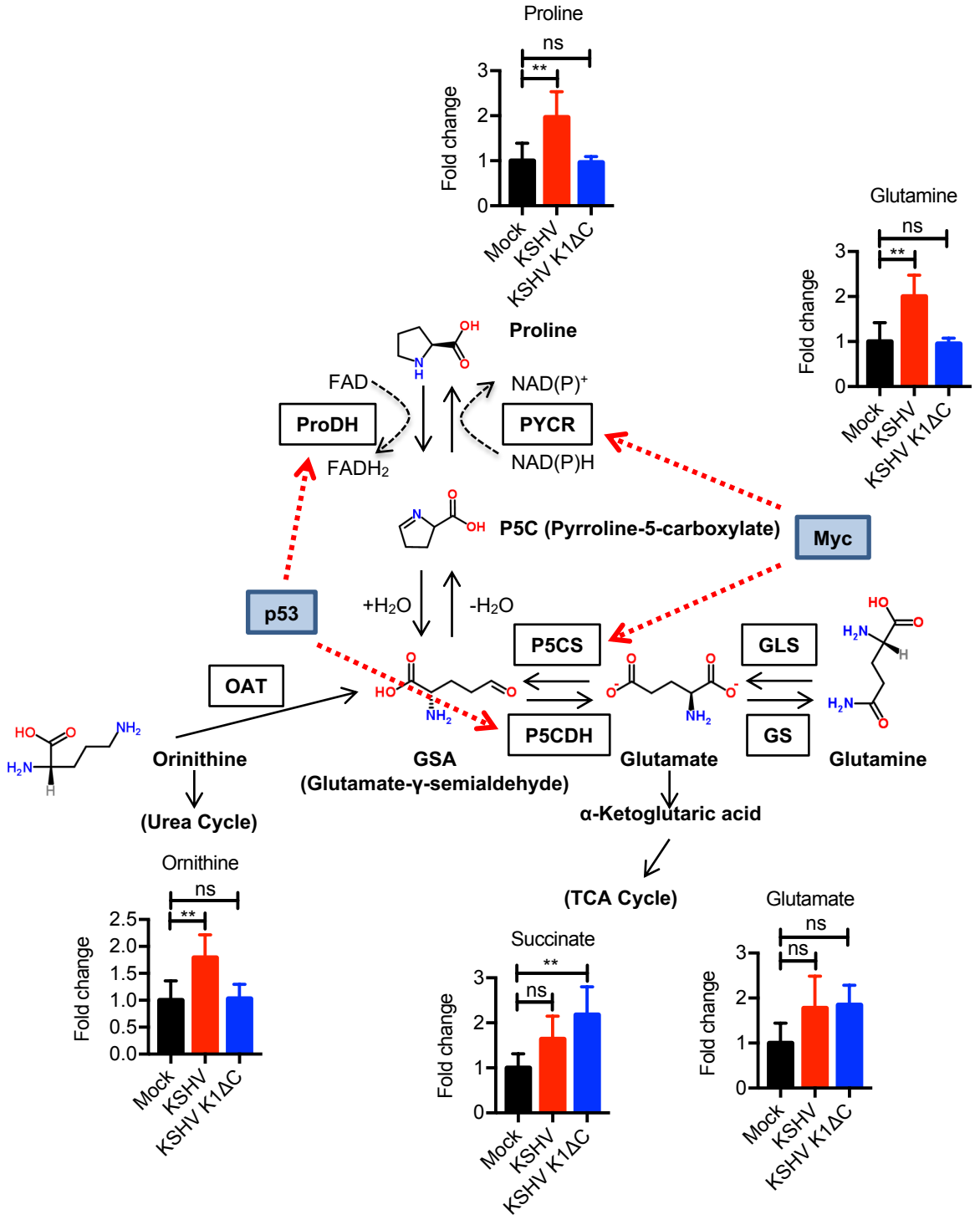

Fig. S7. Stable expression of K1 in TIME, MCF10A and MDA-MB-231 cell lines and Knockdown of PYCR1 and PYCR2 in TIME and KMM cell lines

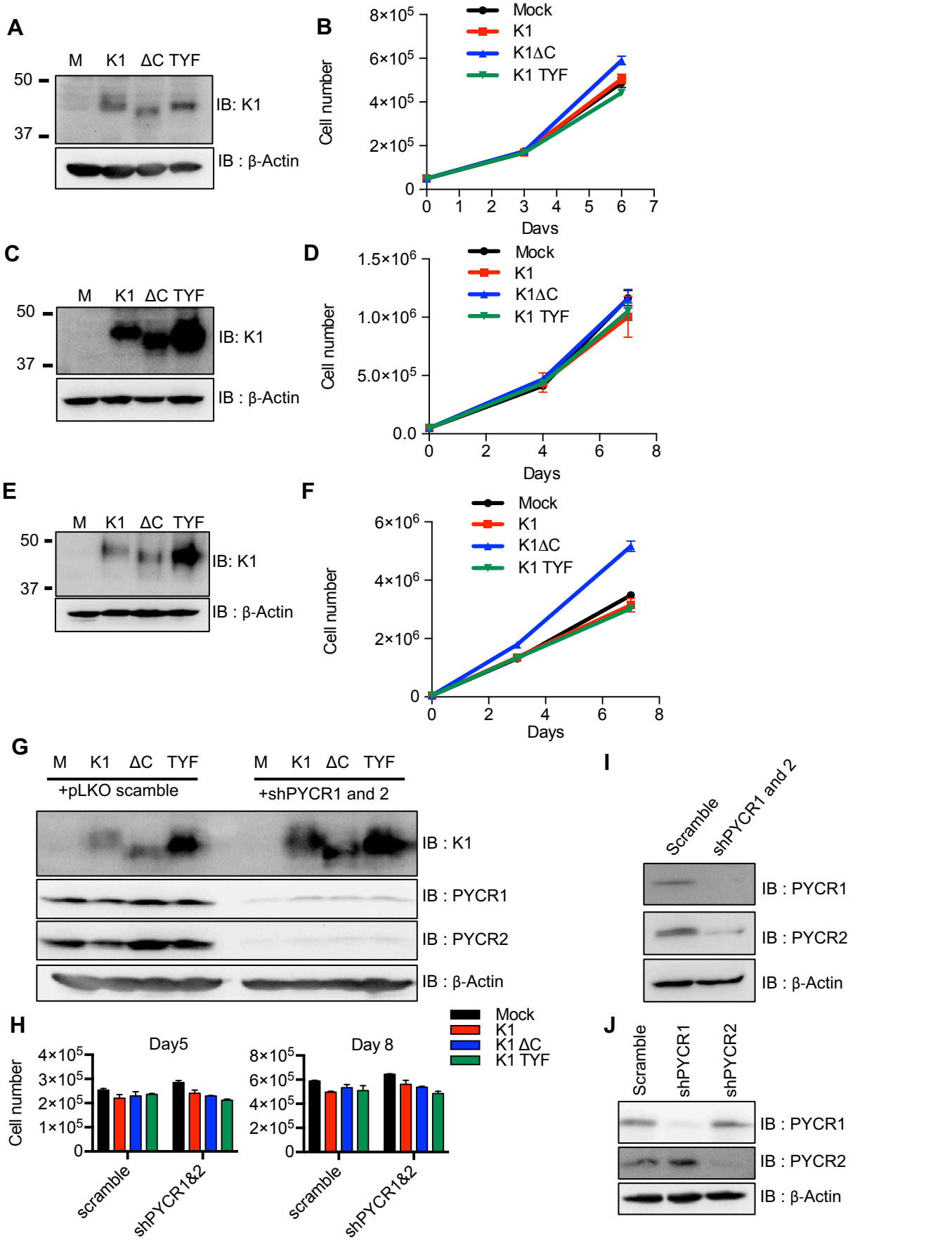

Fig. S8. 3D hydrogel scaffolds for endothelial cell growth

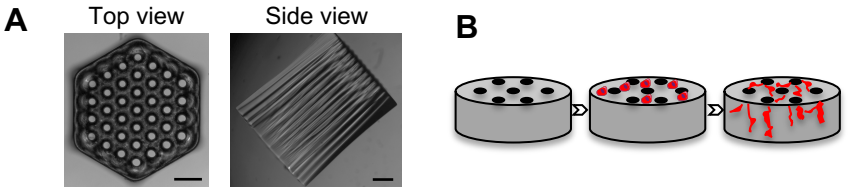

Fig. S9. K1 WT and K1 TYF induce tumorigenesis